SEMARAK ILMU PUBLISHING

Journal of Advanced Research in Fluid Mechanics and Thermal Sciences

Journal homepage:
https://semarakilmu.com.my/journals/index.php/fluid_mechanics_thermal_sciences/index
ISSN: 2289-7879

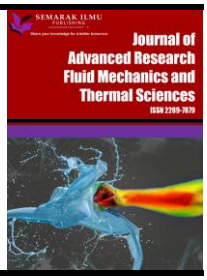

Investigating the Impact of Magnetohydrodynamic (MHD) and Radiation on the Casson-Based Nanofluid Flow over a Linear Stretching Sheet in a Porous Medium with Heat Source or Sink

Ramanjana Koka[1,2,*], Aruna Gajikunta[1]

[1] Department of Mathematics, School of Science, GITAM-Hyderabad Campus, Hyderabad 502329, Telangana, India
[2] Department of Mathematics, St. Francis College for Women, Begumpet, Hyderabad-500016, Telangana, India

ARTICLE INFO

Article history:
Received 13 August 2023
Received in revised form 31 October 2023
Accepted 13 November 2023
Available online 30 November 2023

Keywords:
MHD; Porous media; Casson-based nanofluid; stretching sheet; heat source/sink; thermophoresis; Brownian motion

ABSTRACT

This study delves into the magnetohydrodynamic (MHD) flow of Casson-based nanofluids over a linear stretching sheet, accounting for multiple influencing factors. These findings offer significant real-time applications across a spectrum of fields, including energy generation, environmental engineering, and materials science. The acquired insights into Casson-based nanofluid behaviour within magnetohydrodynamic contexts can foster efficiency improvements, energy conservation, and enhanced overall system and process performance. Furthermore, the current study aims at Casson-based nanofluid's magnetohydrodynamic flow across a linear stretching sheet considering effects of thermal radiation, heat source/sink, and porosity. The governing equations are converted to ordinary differential equations by using similarity transformations. The Runge-Kutta-4 method, along with the shooting technique, is used to solve the reduced equations. The effects of dimensionless parameters, magnetic, Casson, thermophoresis, thermal radiation, and Brownian motion on velocity, thermal, and concentration profiles are considered in the study. As the magnetic and Casson parameters are increased, the findings indicate a reduction in the thickness of the momentum boundary layer. Moreover, the fluid temperature intensifies with the enhancement of thermophoresis and Brownian motion of particles. Finally, for various combinations of applied parameters, the values of skin friction coefficient, Nusselt number, and Sherwood number are obtained and are shown in the tables. The research is unique in a way that incorporates the impacts of heat source/sink and porosity as well as a more precise description of Casson nanofluid flow when compared to earlier findings. The novelty of the investigation lies in the implementation of a heat source/sink and porosity to obtain refined Casson nanofluid flow.

1. Introduction

The investigation of boundary layer flow over a linearly stretching sheet, incorporating heat transfer within a porous medium, has held considerable importance due to its practical applications across both industry and scientific domains. This study led to the development of different materials

* *Corresponding author.*
E-mail address: rkoka@gitam.in

https://doi.org/10.37934/arfmts.111.2.170194

like glass fibres, drawing of copper wires, hot rolling, metal extrusion and spinning etc. A nanofluid comprises a blend of a base fluid and nanoparticles. The diameter of the nanoparticle varies from 1 to 100nm. Base fluids can be glycol, water, toluene, ethylene, etc. Metal oxides, non-metal oxides or carbides are then dispersed in the base fluid to form nanofluid. The main purpose of studying nanofluids is that they increase the thermal characteristics of the liquid. This feature is utilized in double-pane windows, cooling heat exchangers etc.

Fluid hydrodynamics plays a key role which describing the fluid flow through any given medium. Newtonian and Non-Newtonian are two categories in fluid hydrodynamics in which non-Newtonian fluids possess shear rate dependence and shear stress. The scientists and mathematicians made attempts to briefly describe rheological features of the non-Newtonian fluids. The analysis of non-Newtonian fluids was quite complicated because of its highly complex non-linear behaviour. In order to reduce the pumping power, non-Newtonian fluids were used as heat exchangers or coolants. The work by Sakiadis [1] offers an understanding of the behaviour of boundary layers in both Newtonian and Non-Newtonian fluid scenarios. Dharmaiah *et al.,* [2] in their model focused on an incompressible non-Newtonian nanofluid flowing through a cone in a transitory 2-dimensional boundary layer in which both the Arrhenius activation energy and radiation absorption are taken into consideration. Makinde and Aziz [3] conducted a computational investigation concerning the boundary layer flow of non-Newtonian fluid across a linearly stretched sheet. Their findings highlighted a correlation between higher thermophoresis and Brownian motion parameters with an augmentation in thickness of temperature boundary layer. In their work, Kefayati and Bassom [4] have elucidated that the selection of the method heavily relies on the constitutive equation employed for the analysis of non-Newtonian fluids. A thorough examination of laminar fluid flow over a flat surface was undertaken by Khan and Pop [5], who employed similarity solutions to explore various parameters including Lewis number, Prandtl number, Thermophoresis and Brownian Motion parameter. Vedavathi *et al.,* [6] theoretically analysed thermally radiative, non-Darcy, magnetohydrodynamic nanofluid flows over a stretched surface, together with consideration of the effects of thermal conductivity and Arrhenius activation energy.

Jakati *et al.,* [7] examined the effect of Brownian motion and thermophoresis on Maxwell nanofluid flow across a linearly stretched sheet under the influence of an oblique external magnetic field. Ismail *et al.,* [8] conducted a stability analysis, which is performed using the numerical solution to the flow at the stagnation point, heat transfer with MHD, and thermal radiation effects across a shrinking sheet. Vedavathi *et al.,* [9,10] described entropy analysis of thermal convection flow of a nanofluid via inverted cone with suction/injection in a magnetohydrodynamic (MHD) system and Buongiorno's model is used, taking into account Brownian motion and thermophoresis effects.

Reddy *et al.,* [11] explored the unsteady MHD flow considering the viscous dissipation and heat source, whereas Hamid *et al.,* [12] focused on the heat source with the permeable channel. Noor *et al.,* [13] in their work examined the impacts of chemical reaction, thermal radiation, and heat generation/absorption on the magnetohydrodynamic (MHD) Casson nanofluid's heat and mass transport properties along with the effects of viscosity and joule dissipation. There are quite a few non-Newtonian models in the open literature that are discussed by Bhatti *et al.,* [14], Ellahi *et al.,* [15], Alamri *et al.,* [16], and Mabood *et al.,* [17]. On a surface that stretches curves, the MHD extended flow of second-grade viscoelastic nanofluid is investigated by Hosseinzadeh *et al.,* [18].

A porous medium refers to a material or substance that contains interconnected void spaces or pores within its structure. These void spaces can be filled with gases, liquids, or even other solid materials. Porous media is commonly encountered in various natural and engineered systems and plays a crucial role in many scientific and engineering applications. Dinarvand *et al.,* [19] studied mixed convection of a thermos-micropolar binary nanofluid (TMBNF) onto a shrinking and porous

plate investigated using a mass-based hybridity model. Rostami *et al.,* [20] investigated motion and temperature distribution of a hybrid nanofluid composed of a base fluid ethylene glycol and water and nanoparticles made of TiO_2 and MoS_2 in the presence of dust particles in which a magnetic field is influencing the fluid in a porous medium as it flows over a stretched sheet. Dharmaiah *et al.,* [21] examined flow and heat transfer in boundary layer provided to characterise the behaviour of a porous exponentially stretched sheet where Joule dissipation and Activation energy are considered with no-slip conditions.

Among the non-Newtonian fluid types, Casson nanofluid has been largely used in various industrial applications. Casson fluid is a very shear-thinning liquid with incalculable viscosity with an insignificant shear rate. Nanofluids are produced by very minute nanosized particles. In the earlier days, analysis of Casson fluid flow was described by the researchers Kumaran and Sandeep [22], Mohyud-Din *et al.,* [23], Reddy [24], and Hussanan *et al.,* [25]. Nadeem *et al.,* [26] analysed the MHD layer flow of Casson nanofluid with convective boundary conditions. Reyaz *et al.,* [27] examined the impact of heat radiation on the free convection flow of MHD Casson fluid across an oscillating plate, with the Caputo fractional derivative. The impact of heat transfer was investigated by Ramesh *et al.,* [28] in the context of a Casson nanofluid incorporating Cattaneo Christov heat diffusion. Kumar *et al.,* [29] studied the impact of particle deposition for a Casson nanofluid across a thin moving needle. Gudekote and Choudhari [30] also investigated combined effects of slip and inclination on the peristaltic transport of Casson fluid in an elastic tube with porous walls. Tawade *et al.,* [31] also studied the use of heat transfer of Casson transverse the linearly stretched sheet to investigate problem of constant laminar flow of nanofluid on two-dimensional boundary layer. Lately, Abo-Dahab *et al.,* [32] comprehensively reviewed the blowing and suction effect for the flow of Casson nanofluid over an extended surface. The heat transfer associated with the boundary layer flow of Casson fluid induced by a mobile plate within a free stream velocity was examined in the analysis conducted by Mustafa *et al.,* [33]. Numeric solution for the Casson fluid heat transfer over a symmetric wedge was deliberated by Mukhopadhyay *et al.,* [34].

Thermal radiation plays an important role in high-temperature fluid dynamics scenarios, such as combustion, heat exchangers, and the behaviour of gases at extreme temperatures. Understanding and modelling thermal radiation is crucial for accurately predicting temperature distributions and heat transfer in these situations.

Distinct researchers, as cited in the work of Haq *et al.,* [35], Hussain *et al.,* [36], Reddy [37], and Oyelakin *et al.,* [38], have systematically elucidated the theoretical underpinnings of thermal radiation combined with convective boundary conditions. Yusof *et al.,* [39] examined steady-state stagnation point flow and radiative heat transfer of a Casson fluid, a non-Newtonian fluid, over an exponentially permeable slippery Riga plate in the presence of thermal radiation, magnetic field, velocity slip, thermal slip, and viscous dissipation effects.

The heat sources/sinks are fundamental concepts in fluid dynamics that have wide-ranging implications for understanding and controlling the behaviour of fluids in various practical applications. Their proper consideration is essential for achieving efficient and effective heat transfer and thermal management within fluid systems. The effects of exponential space-dependent heat source of dusty Casson fluid flow with three varying geometries of Cattaneo-Christove heat flux were discussed by Mahanthesh *et al.,* [40]. Khan *et al.,* [41], in their work, explained magnetohydrodynamic (MHD) flow of a double stratified micropolar fluid is analysed in the presence of suction, chemical reaction, and heat source effects over a vertical stretching/shrinking sheet. Ibrahim *et al.,* [42] delved into the characteristics of a dissipative convective Casson fluid, considering the influence of heat sources, slip conditions, and chemical reactions. In their model, Gulzar *et al.,* [43] emphasised the importance of hydromagnetic characteristics, magnetohydrodynamics (MHD),

and a heat source or sink in a complex heat-transport system. Khan *et al.,* [44] studied the heat transfer and magnetohydrodynamic (MHD) mixed convection flow of a dual stratified micropolar fluid across a vertical permeable stretching/shrinking sheet with a heat source and chemical reaction.

This investigation centres on the boundary layer dynamics of a Casson nanofluid, considering influence of heat source/sink phenomena while encompassing the presence of a porous medium. The primary objective of this novel investigation lies in comprehending the characteristics of Casson-derived nanofluids, a distinctive class of fluids incorporating nanoparticles and displaying non-Newtonian attributes, while subjected to the impacts of thermal radiation. The work focuses on MHD boundary layer flow across a linear stretching sheet in the steady flow of the nanofluid in the presence of Lorentz force. The general objective of this study is to develop a greater knowledge of the behaviour of non-Newtonian nanofluids when subjected to thermal radiation, which may have implications in a variety of areas, including fluid dynamics and heat transfer.

2. Methodology

2.1 Mathematical Formulation

Consider a steady 2D MHD incompressible, laminar flow of a Casson-based nanofluid in a linear stretching sheet together with effects of radiation and a heat source/sink in a homogeneous porous media. The stretching sheet is aligned along x-axis and the flow is initiated by the stretched sheet as shown in Figure 1. As a result, sheet is stretched by a linear velocity

$$u_w(x) = ax$$

while retaining a stationary origin, where 'a' denotes a positive constant related to the sheet's stretching process.

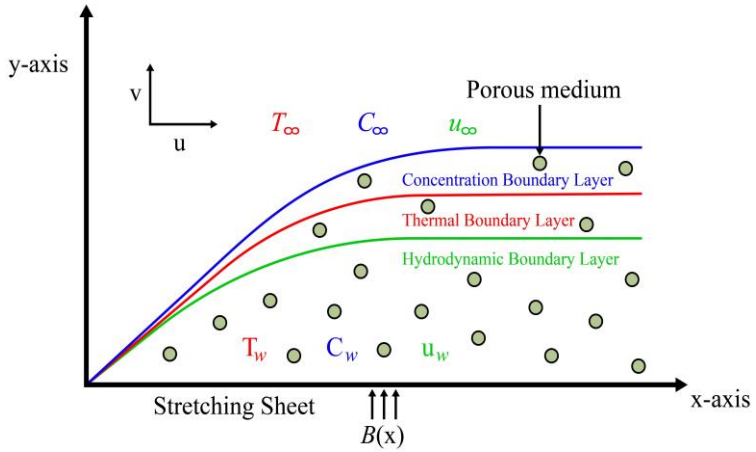

Fig. 1. Flow Geometry

The flow assumptions considered are as follows:

i. Flow is considered $y > 0$.
ii. Magnetic field effect is normal to the direction of flow.
iii. Homogeneous porous medium is considered in fluid flow.
iv. Heat source/sink has been considered along with radiation effect.

The following rheological equation of state for an isotropic, incompressible flow of a Casson fluid is taken from the previous study by Yashkun *et al.,* [45] as follows:

$$\tau_{ij} = \begin{cases} 2\left(\mu_B + \frac{P_y}{\sqrt{2\pi}}\right)e_{ij}, \pi > \pi_c \\ 2\left(\mu_B + \frac{P_y}{\sqrt{2\pi_c}}\right)e_{ij}, \pi_c > \pi \end{cases}$$

Here, $\pi = e_{ij}$, e_{ij} is the $(i,j)^{th}$ component of deformation rate with itself, μ_B is plastic dynamic viscosity of the non-Newtonian fluid, P_y is the fluid's yield stress, and π_c signifies critical value of this product followed by non-Newtonian model.

The governing equations under said conditions are presented below, taken from prior research by Lanjwani *et al.,* [46], with certain modifications:

$$\frac{\partial u}{\partial x} + \frac{\partial u}{\partial y} = 0 \tag{1}$$

$$u\frac{\partial u}{\partial x} + v\frac{\partial u}{\partial y} = \vartheta\left(1 + \frac{1}{\beta}\right)\frac{\partial^2 u}{\partial y^2} - \frac{\sigma B^2}{\rho_f}u - \frac{\vartheta}{K^{**}}u \tag{2}$$

$$u\frac{\partial T}{\partial x} + v\frac{\partial T}{\partial y} = \alpha\frac{\partial^2 T}{\partial y^2} + \tau\left[D_B\frac{\partial C}{\partial y}\frac{\partial T}{\partial y} + \frac{D_T}{T_\infty}\left(\frac{\partial T}{\partial y}\right)^2\right] - \frac{1}{(\rho c)_f}\frac{\partial q_r}{\partial y} + \frac{Q}{(\rho c)_p}(T - T_\infty) \tag{3}$$

$$u\frac{\partial C}{\partial x} + v\frac{\partial C}{\partial y} = D_B\frac{\partial^2 C}{\partial y^2} + \frac{D_T}{T_\infty}\frac{\partial^2 T}{\partial y^2} \tag{4}$$

Eq. (1) is a continuity equation that states inflow and outflow of fluid are equal. Eq. (2) is the momentum equation which preserves law of conservation of momentum. LHS is due to inertial forces, whereas the preceding and final terms are impact of magnetic field and porous media. Eq. (3) states heat or energy equation, LHS term explains convection of heat and RHS third term contributes heat transfer due to a temperature gradient in the y-direction, influenced by the thermal diffusivity of a substance and the temperature difference between the fluid and the surrounding environment. The Last and preceding terms are heat generation/absorbtion and heat flux. Eq. (4), is a concentration equation in which LHS describes how the concentration is being carried along by the fluid flow and RHS's first term represents the diffusive transport of the concentration C due to concentration gradients in the fluid whereas last term indicates thermal diffusion where a potential coupling with temperature varies.

Where Rosseland term is taken from Nagasasikala and Lavanya [47], is expressed as,

$$q_r = -\frac{4\sigma^*}{3K^*}\frac{\partial^2 T}{\partial y^{2\prime}} \tag{5}$$

Here, q_r is radiation term, K^* signifies coefficient of mean absorption and σ^* signifies the Stefan-Boltzmann constant.

Additionally, the streaming for thermal diversity is categorised as free streaming T_∞ and at local temperature T which is assumed to be extremely tiny, series expansions in T^4 using Taylor series expression with T_∞ and rejecting the higher indexes, we get

$$T^4 = 4({T_\infty}^3)T - 3({T_\infty}^4) \tag{6}$$

Using Eq. (5) and Eq. (6), Eq. (3) becomes

$$u\frac{\partial T}{\partial x}+v\frac{\partial T}{\partial y}=\left(\alpha+\frac{16\sigma^{*}}{3K^{*}(\rho c)_{f}}\right)\frac{\partial^{2}T}{\partial y^{2}}+\tau\left[D_{B}\frac{\partial C}{\partial y}\frac{\partial T}{\partial y}+\frac{D_{T}}{T_{\infty}}\left(\frac{\partial T}{\partial y}\right)^{2}\right] \tag{7}$$

with the boundary conditions taken from previous works by Lanjwani *et al.,* [46] and Bakar *et al.,* [48]

$$\left.\begin{aligned} v=0, u=u_{w}(x)=ax, T=T_{w}(x), C=C_{w}(x)\ at\ y=0, \\ u\to 0, T\to T_{\infty}, C\to C_{\infty}\ as\ y\to\infty \end{aligned}\right\} \tag{8}$$

where u and v are velocity components taken along x and y directions, B is Magnetic field, ρ is Density of fluid (kg m^{-3}), c_p is heat capacity (J Kg^{-1} K^{-1}), Kinematic viscosity (m^{2}s^{-1}) is indicated by the symbol ϑ, electrical conductivity (Sm^{-1}) is denoted by the symbol σ and thermal diffusivity (m^{2}s^{-1}) is marked by the symbol α and Casson fluid parameter $\beta=k_c\frac{\sqrt{2\pi_c}}{\tau_0}$ and K^{**} is porous media permeability. Further, T stands for the temperature (K) at the boundary layer, $T_w(x)$ for temperature (K) at the surface, and T_∞ for temperature of free stream (K). The expression $\tau=\frac{(\rho c)_p}{(\rho c)_f}$ is the ratio of heat capacity of nano-sized particles to that of the base fluid, Q is heat generation/absorption coefficient. The coefficients for thermophoresis and Brownian diffusion are denoted as, D_T and D_B respectively. C stands for the boundary layer concentration, $C_w(x)$ for the concentration sheet at the wall, and C_∞ for the concentration of the free stream. The velocity components u and v are expressed as stream functions using the notation.

$u=\frac{\partial\psi}{\partial y}$ and $v=\ \frac{\partial\psi}{\partial x}$,

where, $\psi=\sqrt{a\vartheta}xf(\eta)$, indicated dimensionless stream function and the similarity variable is given by $\eta=\sqrt{\frac{a}{\vartheta}}y$. The proposed similarity transformation results in the velocity components u and v are written as taken from previous literature Lanjwani *et al.,* [46].

$$u=axf'(\eta)\ and\ v=\ -\sqrt{a\vartheta}f(\eta) \tag{9}$$

The changes in temperature and concentration are provided by

$$\theta(\eta)=\frac{T-T_\infty}{T_w-T_\infty}\text{ and }\emptyset(\eta)=\frac{C-C_\infty}{C_w-C_\infty} \tag{10}$$

In this case, $\theta(\eta)$ denotes dimensionless temperature profile, while $\emptyset(\eta)$ denotes dimensionless concentration profile. By using Eq. (9) and Eq. (10) in Eq. (1) to Eq. (8), the following simplified two-point boundary value problem has been generated.

$$\left(1+\frac{1}{\beta}\right)f'''(\eta)+\ f(\eta)f''(\eta)-\ f'^{2}(\eta)-K\,f'(\eta)-Mf'(\eta)=0 \tag{11}$$

$$\frac{1}{Pr}\left(1+\frac{4}{3}R\right)\theta''(\eta)+f(\eta)\theta'(\eta)+Nb\emptyset'(\eta)\theta'(\eta)+Nt\theta'^{2}(\eta)+\lambda\theta(\eta)=0 \tag{12}$$

$$\emptyset"(\eta) + Lef(\eta)\emptyset'(\eta) + \frac{Nt}{Nb}\theta"(\eta) = 0 \tag{13}$$

These equations are subjected to boundary conditions as below,

$$\left.\begin{matrix} f(0) = 0, f'(0) = 1, \theta(0) = 1, \emptyset(0) = 1, \eta \to 0 \\ f'(\eta) \to 0,\ \theta(\eta) \to 0,\ \emptyset(\eta) \to 0, \eta \to \infty \end{matrix}\right\} \tag{14}$$

where the dimensionless parameters are, $R = \frac{4\sigma}{K^*\alpha(\rho c)_f}$ is radiation parameter, $M = \frac{\sigma B^2}{\rho_f a}$ magnetic parameter, $K = \frac{v}{K^{**}a}$ is porosity parameter, Prandtl number $Pr = \frac{\vartheta}{\alpha}$, Brownian motion parameter $Nb = \frac{D_B(\rho c)_p(C_w - C_\infty)}{\vartheta(\rho c)_f}$, thermophoresis parameter $Nt = \frac{D_T(\rho c)_p(T_w - T_\infty)}{\vartheta(\rho c)_f T_\infty}$, the heat source or sink parameter $\lambda = \frac{Q}{a(\rho c)_p}$, and Lewis number $Le = \frac{\vartheta}{D_B}$. The following equations are used to calculate the other physical variables, such as the local skin-friction coefficient, the local Nusselt, and the Sherwood numbers respectively are given by

$$C_f = \frac{[\vartheta\left(1+\frac{1}{\beta}\right)\frac{\partial u}{\partial y}]_{y=0}}{\rho {u^2}_w},\ N_u = \frac{-x[\left(\frac{16\sigma^* {T_\infty}^3}{3K^*}+k\right)\frac{\partial T}{\partial y}]_{y=0}}{(T_w - T_\infty)},\ S_h = \frac{-x[\left(\frac{\partial C}{\partial y}\right)]_{y=0}}{(C_w - C_\infty)} \tag{15}$$

By using Eq. (2) to Eq. (7) in Eq. (15), we get the following numbers as

$$C_f\left(\sqrt{Re_x}\right) = \left(1 + \frac{1}{\beta}\right) f''(0),\ N_u\left(\frac{1}{\sqrt{Re_x}}\right) = -(1 + \frac{4}{3}R)\theta'(0),\ S_h\left(\frac{1}{\sqrt{Re_x}}\right) = -\emptyset'(0) \tag{16}$$

where $Re_x = \frac{ax^2}{\vartheta}$ is the Reynolds number.

3. Numerical Analysis

The built-in method NDSolve in MATHEMATICA is used to numerically solve the system of Eq. (11) to Eq. (13) with subjective boundary conditions (14) taken from previous research Yasmin and Nisar [49]. This method is highly sophisticated and effective for solving differential equations. It can deal with a variety of differential equations, including boundary value problems and ordinary differential equations (ODEs). To provide precise results, it uses high-precision numerical methods. To guarantee accurate findings, it makes use of complex numerical algorithms, adaptive step-size control, and error estimates. This section examines how the velocity, heat transfer rate, and concentration are affected by a number of embedded factors.

By using the numerical method Runge-Kutta-4 with shooting technique from previous study Noor *et al.,* [13], we analyze the flow model for solving the ODEs from Eq. (11) to Eq. (14) with the appropriate boundary conditions Eq. (12) over a range of values of the relevant parameters M, K^*, Pr, Nt, Nb, R, Le and λ. The boundary value problem has been transformed into initial value problem by using following parameters as:

$$f = f_1, f' = f_2, f'' = f_3, \theta = f_4, \theta' = f_5, \emptyset = f_6, \emptyset' = f_7.$$

Consequently, the equations are transformed into,

$$f_1' = f_2, f_2' = f_3,$$

$$f_3' = -\left(\frac{-[f_2^2 - f_1 f_3] - K f_2 - M f_2}{\left(1+\frac{1}{\beta}\right)}\right), f_4' = f_5,$$

$$f_5' = -\frac{Pr}{\left(1+\frac{4}{3}R\right)}\left(f_1 f_5 + Nb f_5 f_7 + Nt {f_5}^2 + \lambda f_4\right),$$

The reduced boundary conditions are given as:

$$f_2(0) = 1, f_1(0) = 0, f_4(0) = 1, f_6(0) = 1,$$

$$f_2(\infty) \to 0, f_4(\infty) \to 0, f_6(\infty) \to 0.$$

To implement the RK-4 (Runge-Kutta) process effectively, a finite domain of $0 \leq \eta \leq \infty$ is essential. The choice of an appropriate value for ∞ in the current model depends on the specific values of relevant parameters. For this instance, η_∞ is considered to be less than 10. Once the convergence requirement is met, the set of ordinary differential equations that results is resolved using the RK procedure along with the shooting technique. The advantage of this numerical method is that they can handle complex system of equations provide insights to the behaviour of fluid flow which may not be easily attainable through analytical methods. This approach helps in obtaining the desired solution with the given parameter set. The entire process is then repeated iteratively until the obtained results satisfy the convergence criterion, reaching the desired level of accuracy, which is set at 10^{-6}.

4. Results and Discussion

The study investigates the non-linear steady-state boundary layer, heat and mass transfer of an incompressible laminar Casson nanofluid flow passing across a linearly stretching sheet. We compute numerically acquired values for velocity profile $f'(\eta)$, temperature or thermal profile $\theta(\eta)$, and concentration profile $\phi(\eta)$ in order to assess the physical importance of the issue. The computations involve pertinent parameters, such as Casson parameter β, radiation parameter R, magnetic parameter M, thermophoresis parameter Nt, Brownian motion parameter Nb, Prandtl number Pr, and Lewis number Le. For authentication purposes, the results which are obtained numerically are compared with the values of skin friction reported by Khan and Pop [5] and Ferdows *et al.,* [50], in Table 1. The results exhibit strong consistency with recently acquired data, instilling a sense of assurance in the precision of the current methodology. Table 2 and Table 3 present values of skin friction coefficient and heat and concentration transfer rates.

The results demonstrate a favourable agreement with the newly obtained data, thereby instilling confidence in the accuracy of current method.

Table 1
We compared our findings to those previously published results as $\beta \to \infty, M = R = 0$

$Nb = Nt$	Khan and Pop *et al.,* [5]	Ferdows *et al.,* [50]	Present results
0.1	0.9525	0.9524	0.95835
0.2	0.3654	0.3653	0.37855
0.3	0.1355	0.1351	0.13381
0.4	0.0495	0.0490	0.04233
0.5	0.0179	0.0178	0.01913

Table 2
Results for various values of dimensionless parameters for local skin friction, Local Nusselt number, and Sherwood number

β	M	Pr	Nt	Le	Nb	R	$f''(0)$	$-\theta'(0)$	$-\emptyset'(0)$
∞							-1.0000622	0.49545971	0.2618811
0.5							-0.5786731	0.56966433	0.3574765
1	0						-0.70760123	0.54671042	0.3260212
	0.5						-0.86607110	0.51873124	0.2896772
	1	1					-1.00000521	0.49555200	0.2619361
		3					-1.00000521	0.85113165	-0.0098410
		7.5	0.2				-1.00000521	1.152321224	-0.2497094
			0.3				-1.00000521	1.024231732	-0.4905012
			0.5	1			-1.00000521	0.81040739	-0.7268871
				2			-1.00000521	0.54656577	-0.4158094
				3	0.2		-1.00000521	0.43251464	1.01889115
					0.3		-1.00000521	0.30072181	1.22871297
					0.5	0	-1.00000521	0.13440125	1.31005918
						0.5	-1.00000521	0.24054516	1.20984192
						1	-1.00000521	0.29861256	1.14759579

Table 3
Results for K and λ values of dimensionless parameters for local Skin friction, local Nusselt number, and Sherwood number

K	λ	$f''(0)$	$-\theta'(0)$	$-\emptyset'(0)$
0		-1.00008502	0.335627	
0.5		-1.11854980	0.271591	
1		-1.22475072	0.122671	
	0.1		0.335627	2.1490678
	0.3		0.243797	2.2825742
	0.5		0.169339	2.6985216

Figure 2(a) illustrates velocity profile $f'(\eta)$, decreases with increase in Casson parameter β. As the Casson parameter β increases, fluid viscosity also increases due to applied stress, resulting in a deceleration of the nanofluid flow along the x-axis. Consequently, both velocity and boundary layer thickness decrease. Figure 2(b) gives the comparison graph of velocity profile $f'(\eta)$, temperature profile $\theta(\eta)$, concentration profile $\emptyset(\eta)$ when $\beta \to \infty$.

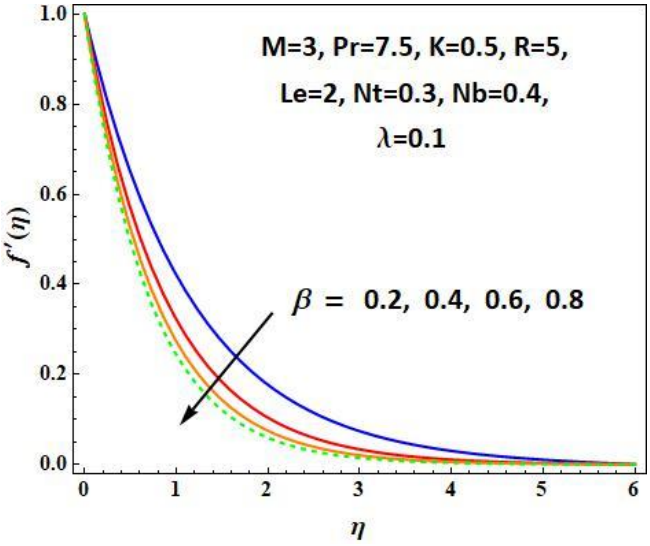

(a)

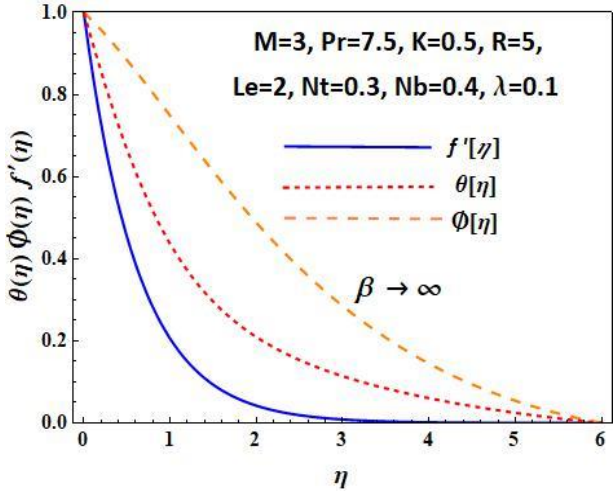

(b)

Fig. 2. (a) The effects of β on velocity profile $f'(\eta)$, (b) The comparison of velocity profile $f'(\eta)$, temperature profile $\theta(\eta)$, concentration profile $\emptyset(\eta)$ when $\beta \to \infty$

In Figure 3, velocity profile $f'(\eta)$ decreases with augmentation of the magnetic parameter M, the influence of Lorentz forces intensifies perpendicular to the x-axis. Consequently, the nanofluid's flow encounters heightened resistance, resulting in a diminished velocity. Importantly, the reduction in nanofluid velocity is observed at close proximity to the sheet in both scenarios, irrespective of whether β or M is increased.

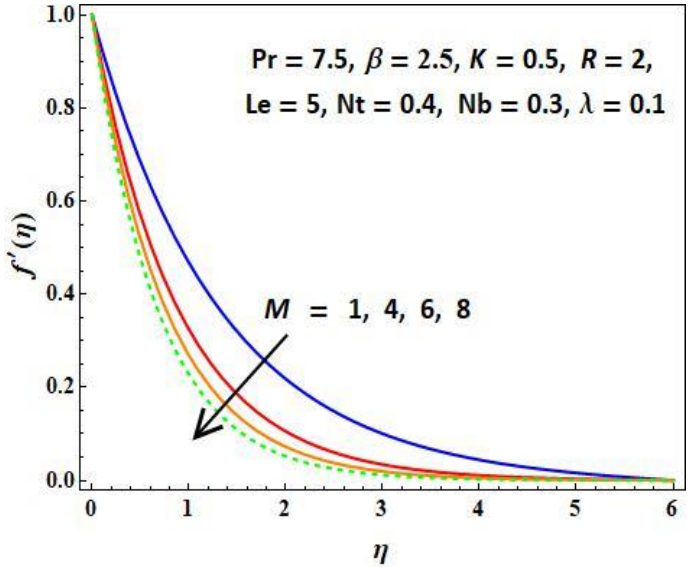

Fig. 3. The effects of *M* on velocity profile $f'(\eta)$

Figure 4 and 5 demonstrate an increase in the Casson fluid parameter β leads to higher temperature $\theta(\eta)$ and concentration $\emptyset(\eta)$ distribution profiles. This physical phenomenon occurs because larger values of β signify stronger molecular motion and interactions, resulting in elevated fluid temperature and concentration rates. As a result, there is an expansion in thickness of thermal and concentration boundary layers.

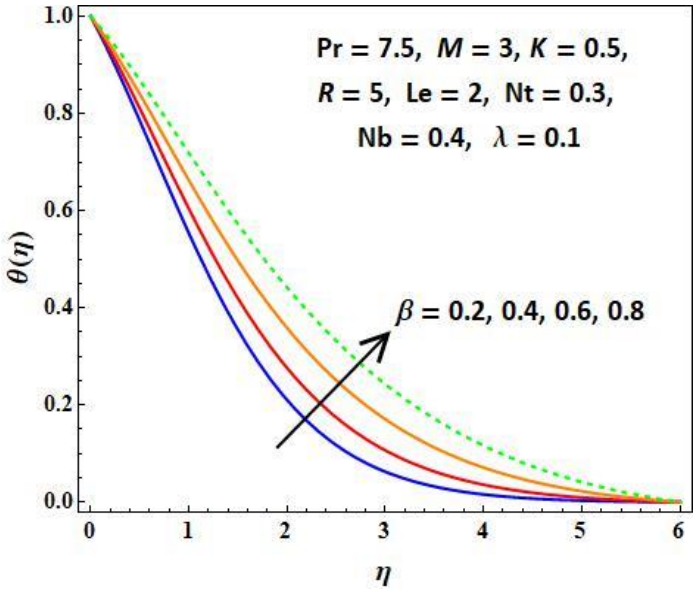

Fig. 4. The effects of β on Temperature profile $\theta(\eta)$

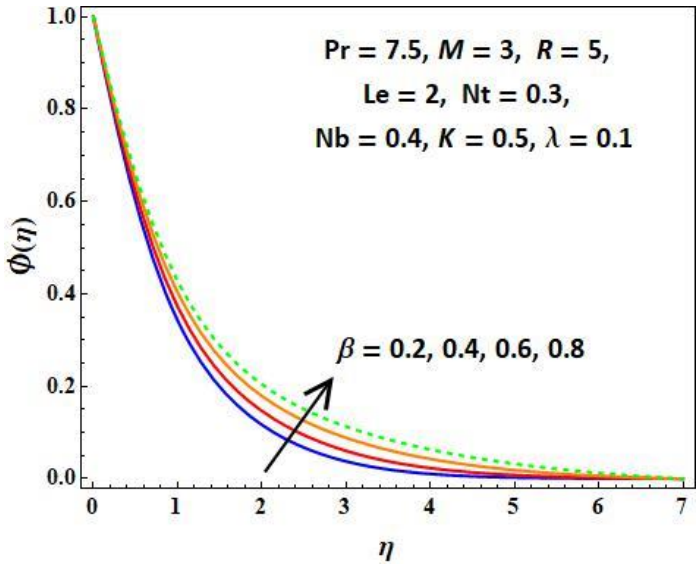

Fig. 5. The effects of β on Concentration profile $\emptyset(\eta)$

In Figure 6, the impact of porosity parameter K on velocity profile $f'(\eta)$ is depicted. Upon utilizing elevated values of K, they have a detrimental effect on the velocity profile as it is taken from previous studies by Ullah *et al.,* [51] and Das *et al.,* [52]. As porosity K increases, the fluid velocity decreases because the wider holes in the porous medium cause the fluid to experience drag, resulting a decline in the width of velocity boundary layer.

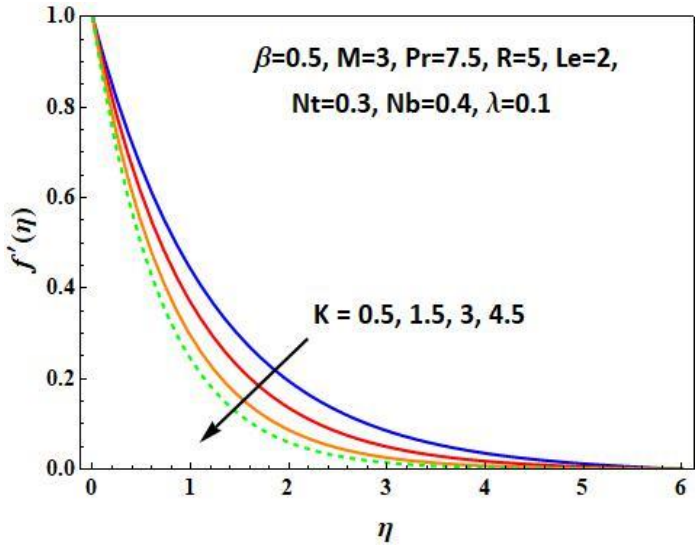

Fig. 6. The effects of K on velocity profile $f'(\eta)$

Figure 7, show impact of porosity parameter K on temperature profile $\theta(\eta)$. As K enhances, the temperature profile $\theta(\eta)$ also increases. This phenomenon can be explained by the escalating viscosity of the liquid as K increases, resulting in a gradual reduction in the liquid's velocity. The higher viscosity exerts greater control over the liquid's movement across the surface. In summary, the variation of the porosity parameter K has a significant impact on the $\theta(\eta)$, temperature profile. Elevated K values induce greater viscosity within the liquid, triggering a decrease in its velocity. As a consequence, this gives rise to a more pronounced thermal boundary layer and an elevated temperature profile along the surface. Figure 7 displays the variations in heat profiles for various porous medium parameters. A porous medium is a solid or group of solids with enough spaces

between them or around them to let a liquid to travel through or around them. As a result, the surface area of the porous media increases when porous media parameter is raised from 0.5 to 4.5, which raises temperature profile.

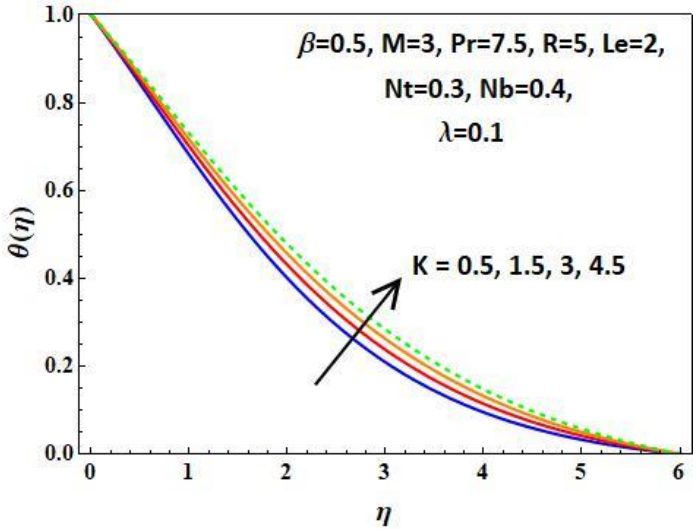

Fig. 7. The effects of K on Temperature profile $\theta(\eta)$

Similar trends are apparent in Figure 8 and 9 as the magnetic parameter M experiences escalation, leading to heightened Lorentz forces. As a result, the temperature $\theta(\eta)$ and concentration $\emptyset(\eta)$ profiles exhibit augmentation, causing a rise in the thickness of thermal and concentration boundary layers.

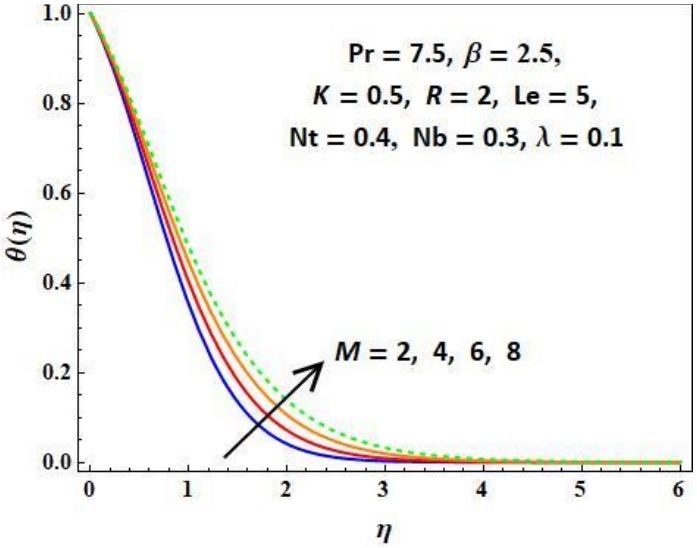

Fig. 8. The effects of M on Temperature profile $\theta(\eta)$

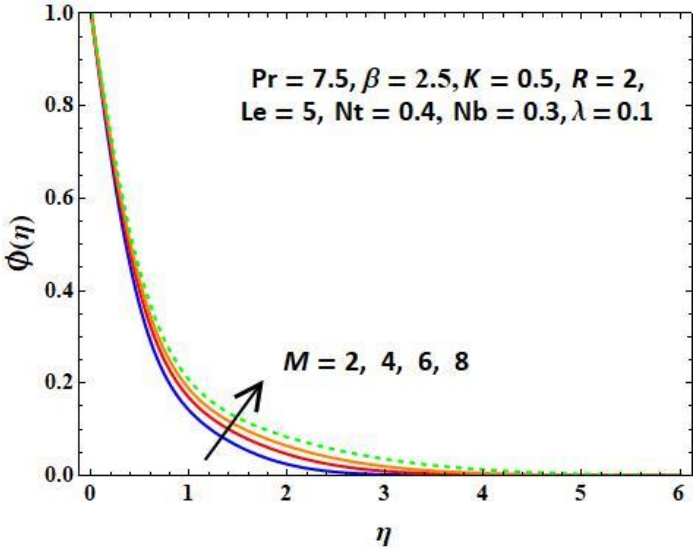

Fig. 9. The effects of M on Concentration profile $\emptyset(\eta)$

In Figure 10, the temperature distribution profile $\theta(\eta)$ is depicted, computed for various Prandtl number Pr values. Since the Prandtl number Pr is inversely correlated with thermal diffusivity, an escalation in its value implies diminished thermal diffusivity, resulting in temperature reduction. Consequently, the thermal boundary layer experiences thinning.

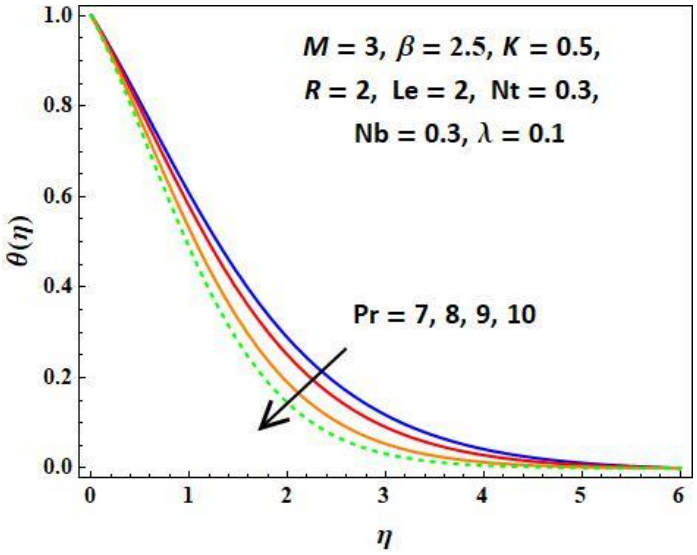

Fig. 10. The effects of Pr on temperature profile $\theta(\eta)$

Figure 11 demonstrates that temperature of nanofluid increases with an enhancement in value of Brownian motion Nb. However, in Figure 12, a contrary tendency is seen for the concentration profile $\emptyset(\eta)$. With increases in Brownian motion parameter Nb, as a result, the thickness of the thermal boundary layer grows as shown in Figure 11, while thickness of concentration boundary layer shrinks shown in Figure 12. This phenomenon is attributed to Brownian motion, which occurs in a zig-zag path, leading to an increase in particle kinetic energy and a subsequent rise in particle collisions.

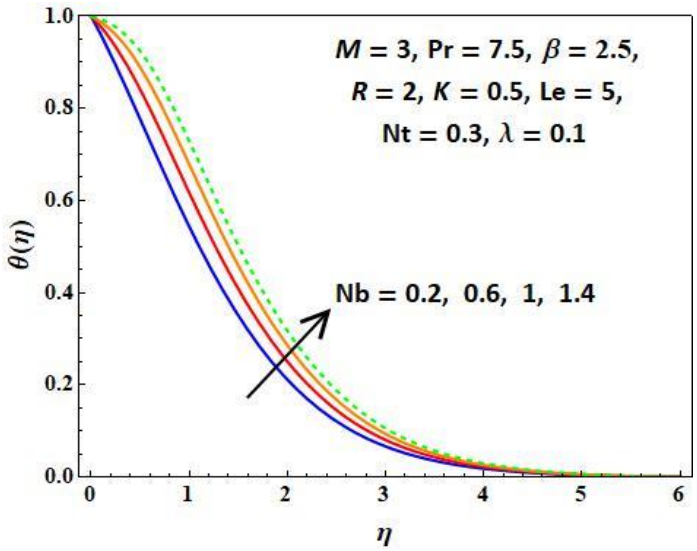

Fig. 11. The effects of Nb on temperature profile $\theta(\eta)$

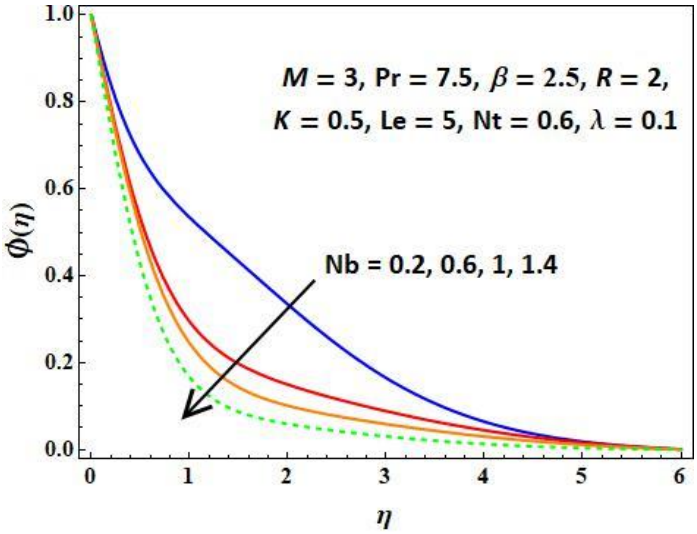

Fig. 12. The effects of Nb on concentration profile $\emptyset(\eta)$

Figure 13 illustrates how the thermophoresis parameter Nt affects the temperature distribution profile $\theta(\eta)$. Due to the thermophoretic effect, caused by the temperature gradient, nano particles are shifted from the hotter stretched sheet to the cooler ambient fluid. As a result, the $\theta(\eta)$ exhibits a cumulative trend with Nt. The boundary layer thickness of temperature is increased as a consequence of thermophoresis strong influence spreading across a broader area of the fluid that contains suspended nanoparticles.

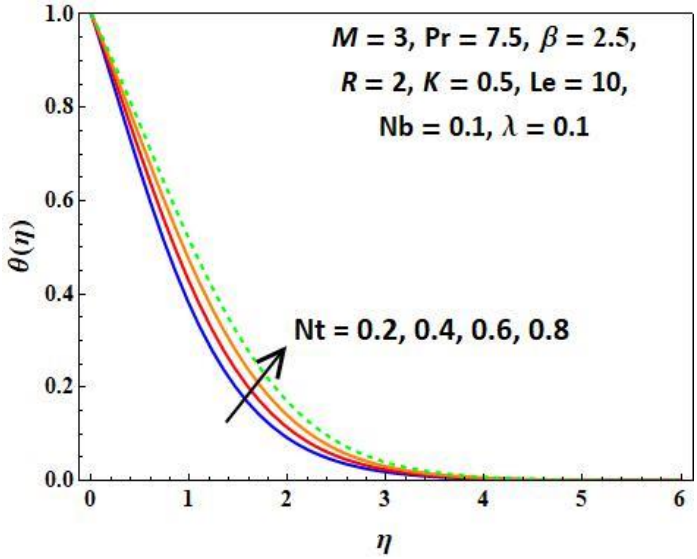

Fig. 13. The effects of Nt on Temperature profile $\theta(\eta)$

Figure 14 indicates a direct proportionality between the concentration of nanoparticles $\emptyset(\eta)$ and the thermophoresis parameter Nt. This relationship arises because an increase in Nt leads to deeper diffusion penetration into the fluid, resulting an increase in the thickness of boundary layers of temperature as well as concentration.

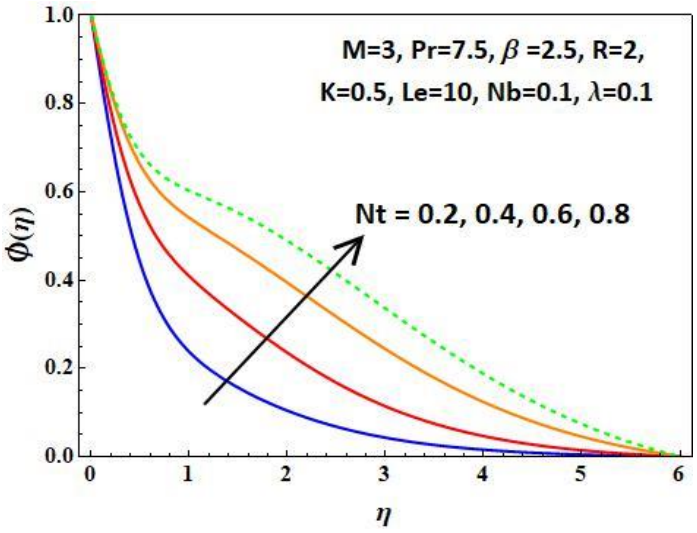

Fig. 14. The effects of Nt on Concentration profile $\emptyset(\eta)$

In Figure 15, the effects of temperature profile on $\theta(\eta)$ results in variation in the dimensionless heat source or sink coefficient λ. When a heat source is present within the fluid flow, it frequently elevates the fluid's overall thermal state. Here $\lambda < 0$ depicts heat sink and $\lambda > 0$ for heat source.

As shown in the figure, the temperature profile $\theta(\eta)$ exhibits an increasing behaviour when the value of the dimensionless heat source/sink coefficient λ is raised within the range of $(\lambda < 0)$, specifically from -0.3 to -0.1 and there is a similar trend is shown in temperature profile $\theta(\eta)$ as λ is further increased within the range of $(\lambda > 0)$, particularly from 0.1 to 0.3 taken from previous study Deepika *et al.,* [53].

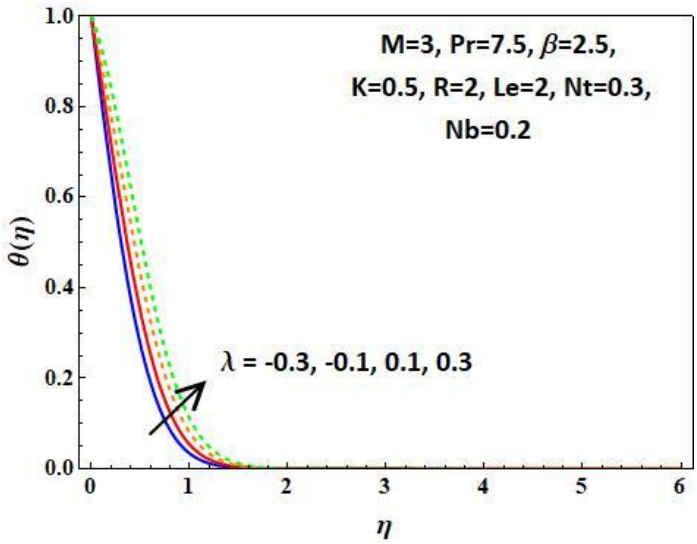

Fig. 15. The effects of λ on Temperature profile $\theta(\eta)$

Figure 16 shows impact of radiation parameter on temperature profile $\theta(\eta)$. The graphic depicts that the fluid temperature rises as *R* increases. This effect happens as a result of a divergence in the radiative heat flux caused by a drop in the mean absorption coefficient K^* at higher levels of R. Thus, the heat transfer rate to the nanofluid is elevated as the radiation parameter continuously releasing heat energy into the flow zone, raising the temperature of the nanofluid.

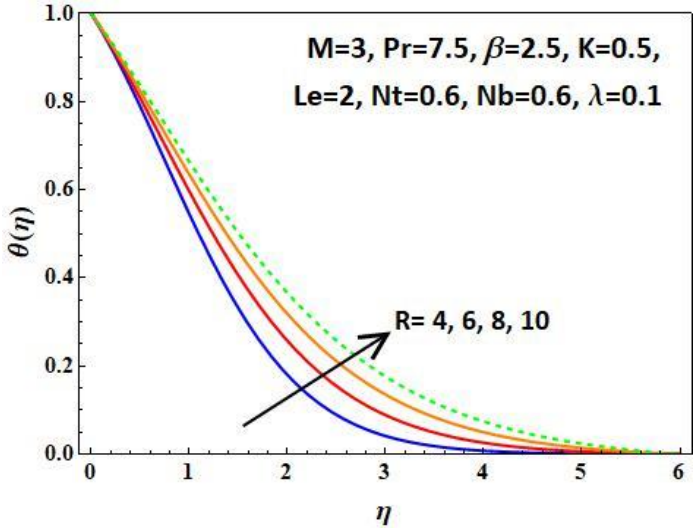

Fig. 16. The effects of R on Temperature profile $\theta(\eta)$

The impact of Lewis number Le on concentration profile $\emptyset(\eta)$ of the nanoparticles is shown in Figure 17. The analysis demonstrates that thickness of concentration boundary layer reduces as Lewis number Le rises. This effect occurs due to the higher Lewis number Le leading to an increase in the concentration rate of nanoparticles, resulting a decrease in the concentration profile $\emptyset(\eta)$.

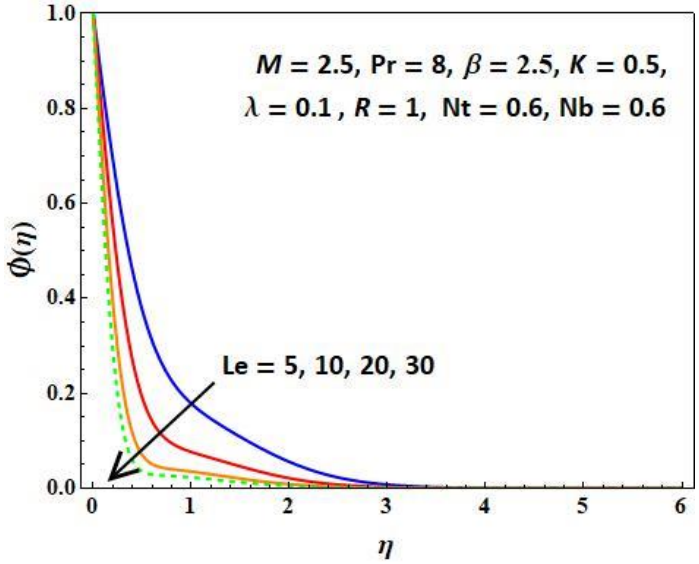

Fig. 17. The effects of Le on Concentration profile $\emptyset(\eta)$

In Figure 18, it is evident that an increase in heat source/sink parameter λ results in enhanced concentration diffusion, while a decrease in λ leads to enhanced mass diffusion where the similar results were obtained in the literature of Hsiao [54].

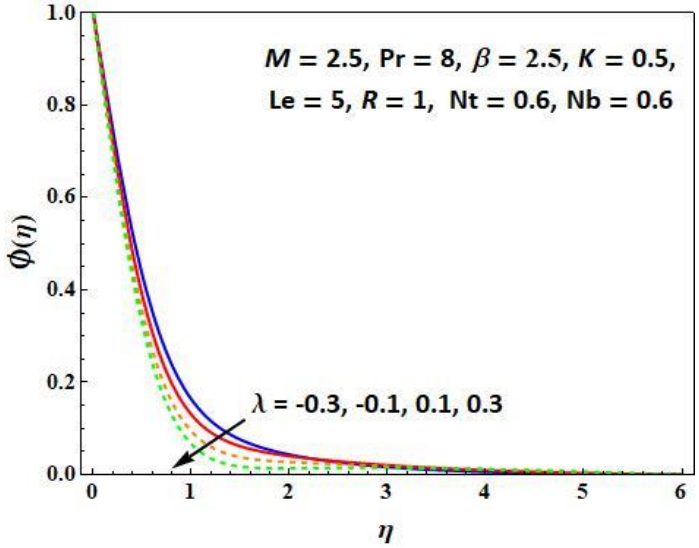

Fig. 18. The effects of λ on Concentration profile $\emptyset(\eta)$

The concentration profile's $\emptyset(\eta)$ combined response to the radiation parameter R and Lewis number Le is depicted in Figure 19. The plot indicates as a rise in both the radiation parameter R and Lewis number Le leads to decrease in concentration rate. Consequently, species boundary layer reduces.

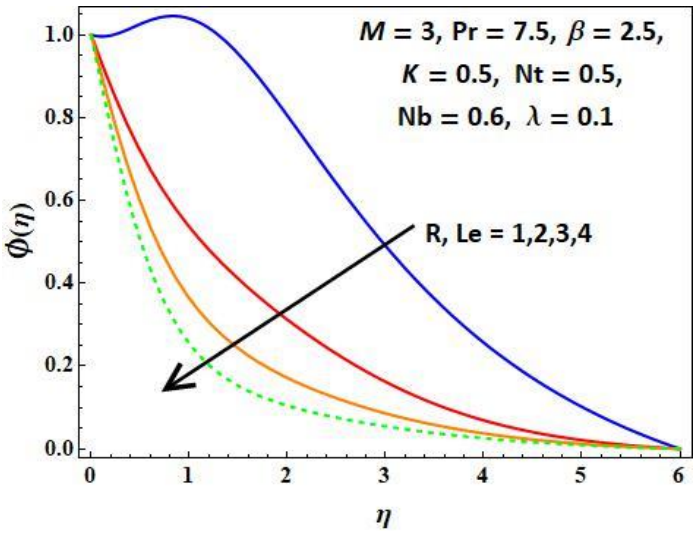

Fig. 19. The effects of R, Le on Concentration profile $\emptyset(\eta)$

Figure 20 and 21 display the impact of the thermophoresis Nt on heat transfer rate and concentration transfer rates. As thermophoresis parameter, Nt upsurges, rate of heat transfer declines. Conversely, the concentration rate improves with an upsurge in the thermophoresis parameter.

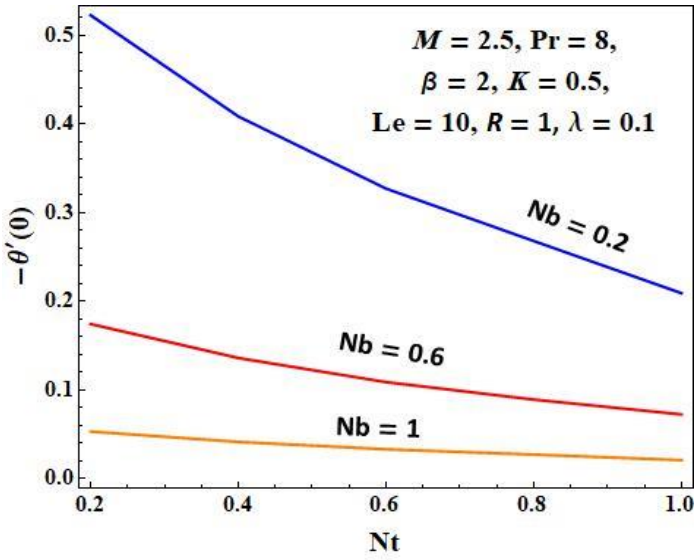

Fig. 20. The effects of Nt on Nusselt Number

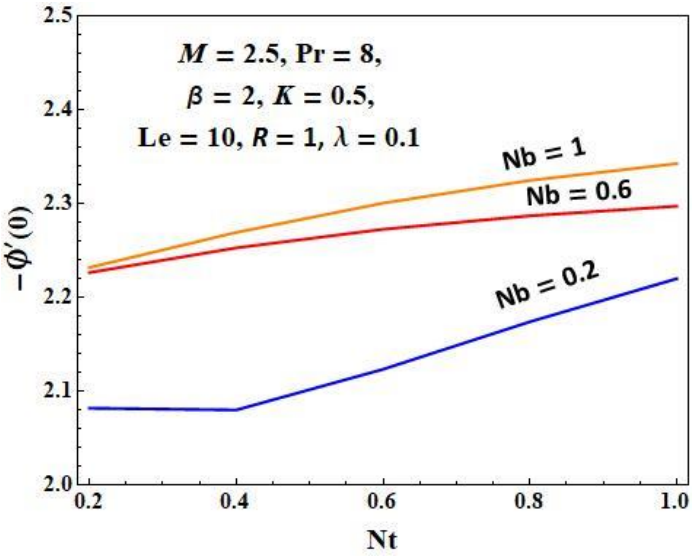

Fig. 21. The effects of Nt on Sherwood Number

The impact of Brownian motion Nb on heat and concentration transport is seen in Figure 22 and 23. The results show that the heat transfer rate reduces as Brownian motion rises, but the concentration rate exhibits the reverse tendency.

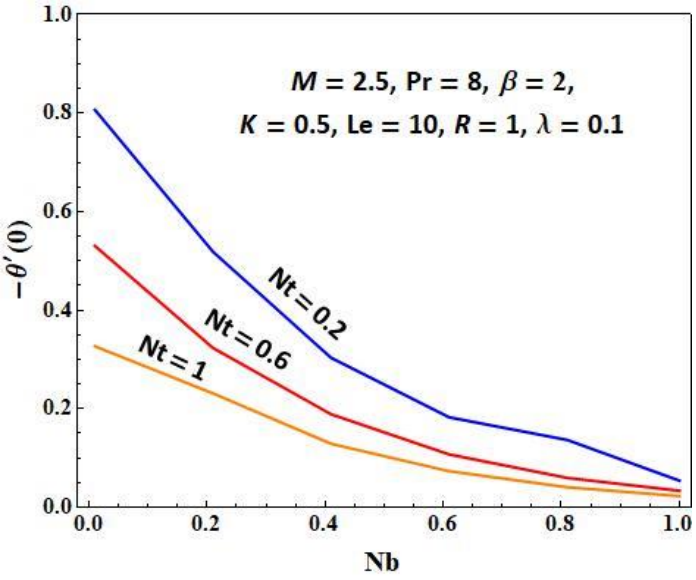

Fig. 22. The effects of Nb on Nusselt Number

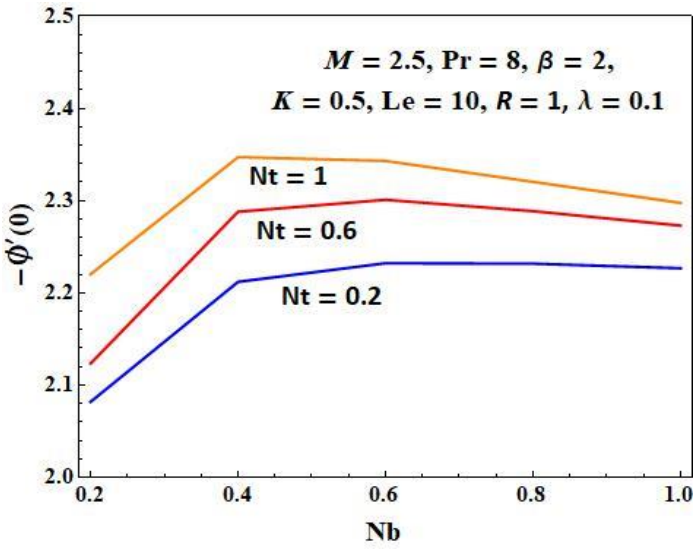

Fig. 23. The effects of Nb on Sherwood Number

5. Conclusions

The current work studies the Casson nanofluid flow across a linear stretching sheet in the boundary layer in a porous medium along with heat source/sink. The following list summarises the main conclusions of this study:

i. As the values of Casson parameter β and magnetic parameter M increase, velocity decreases. However, simultaneously, the rates of heat transfer and concentration transfer increase.
ii. As higher values of Porosity parameter K are employed, they have a ruinous effect on the velocity profile. As the value of K increases, significantly it raises thermal boundary layer thickness.
iii. A rise in the Prandtl number Pr led to a reduction in the rate of heat transfer.
iv. An increase in the rate of thermal radiation R results in an increase in rate of temperature distribution.
v. Enhancing the values of heat source/sink λ led to reduction of thermal boundary layer thickness.
vi. When heat source/sink parameter λ is intensified, mass diffusion is enhanced, whereas reducing the λ values encourage concentration diffusion.
vii. An upsurge in the thermophoresis parameter Nt and the Lewis number Le led to an increase in both the rate of temperature as well as the rate of concentration.
viii. As the Lewis number Le and the radiation parameter R combined effects, amplify heat transfer rates, but concurrently lead to a reduction in concentration or volume fraction rates.
ix. Temperature rises as the Brownian factor Nt grows, yet concentration rates decline in response.
x. While altering Nt or Nb across diverse values, heat transfer escalates, yet the pace of concentration dwindles.

The researchers are motivated to simulate 3D Casson-based nanofluid flow, mass, and heat transfer issues that are related to the areas of mechanical engineering using the present CFD simulation. It may be used to investigate a variety of issues pertaining to chemical engineering, solar collectors, pharmaceuticals, medical fields, thermal industries, etc. The current issue offers an

exciting opportunity to show how a tri-hybrid nanofluid flows through horizontally extending sphere, cylinder, cone, and other surfaces while being subjected to various physical influences.

Acknowledgement
This research was not funded by any grant.

References

[1] Sakiadis, B. C. "Boundary-layer behavior on continuous solid surfaces: II. The boundary layer on a continuous flat surface." *AIChE Journal* 7, no. 2 (1961): 221-225. https://doi.org/10.1002/aic.690070211
[2] Dharmaiah, G., S. Dinarvand, P. Durgaprasad, and S. Noeiaghdam. "Arrhenius activation energy of tangent hyperbolic nanofluid over a cone with radiation absorption." *Results in Engineering* 16 (2022): 100745. https://doi.org/10.1016/j.rineng.2022.100745
[3] Makinde, Oluwole D., and A. Aziz. "Boundary layer flow of a nanofluid past a stretching sheet with a convective boundary condition." *International Journal of Thermal Sciences* 50, no. 7 (2011): 1326-1332. https://doi.org/10.1016/j.ijthermalsci.2011.02.019
[4] Kefayati, Gholamreza, and Andrew P. Bassom. "A lattice Boltzmann method for single-and two-phase models of nanofluids: Newtonian and non-Newtonian nanofluids." *Physics of Fluids* 33, no. 10 (2021). https://doi.org/10.1063/5.0067744
[5] Khan, W. A., and I. Pop. "Boundary-layer flow of a nanofluid past a stretching sheet." *International Journal of Heat and Mass Transfer* 53, no. 11-12 (2010): 2477-2483. https://doi.org/10.1016/j.ijheatmasstransfer.2010.01.032
[6] Vedavathi, N., Ghuram Dharmaiah, Kothuru Venkatadri, and Shaik Abdul Gaffar. "Numerical study of radiative non-Darcy nanofluid flow over a stretching sheet with a convective Nield conditions and energy activation." *Nonlinear Engineering* 10, no. 1 (2021): 159-176. https://doi.org/10.1515/nleng-2021-0012
[7] Jakati, Sushma V., Raju B. T., Achala L. Nargund, and S. B. Sathyanarayana. "Study of Maxwell nanofluid flow over a stretching sheet with non-uniform heat source/sink with external magnetic field." *Journal of Advanced Research in Fluid Mechanics and Thermal Sciences* 55, no. 2 (2019): 218-232.
[8] Ismail, Nurul Syuhada, Yong Faezah Rahim, Norihan Md Arifin, Roslinda Nazar, and Norfifah Bachok. "Stability analysis of the stagnation-point flow and heat transfer over a shrinking sheet in nanofluid in the presence of MHD and thermal radiation." *Journal of Advanced Research in Fluid Mechanics and Thermal Sciences* 91, no. 2 (2022): 96-105. https://doi.org/10.37934/arfmts.91.2.96105
[9] Vedavathi, N., Gurram Dharmaiah, Shaik Abdul Gaffar, and Kothuru Venkatadri. "Entropy analysis of magnetohydrodynamic nanofluid transport past an inverted cone: Buongiorno's model." *Heat Transfer* 50, no. 4 (2021): 3119-3153. https://doi.org/10.1002/htj.22021
[10] Vedavathi, N., Gurram Dharmaiah, Shaik Abdul Gaffar, and Kothuru Venkatadri. "Entropy analysis of nanofluid magnetohydrodynamic convection flow past an inclined surface: a numerical review." *Heat Transfer* 50, no. 6 (2021): 5996-6021. https://doi.org/10.1002/htj.22159
[11] Reddy, Machireddy Gnaneswara, Polarapu Padma, and Bandari Shankar. "Effects of viscous dissipation and heat source on unsteady MHD flow over a stretching sheet." *Ain Shams Engineering Journal* 6, no. 4 (2015): 1195-1201. https://doi.org/10.1016/j.asej.2015.04.006
[12] Hamid, M., M. Usman, Z. H. Khan, Rizwan Ul Haq, and W. Wang. "Numerical study of unsteady MHD flow of Williamson nanofluid in a permeable channel with heat source/sink and thermal radiation." *The European Physical Journal Plus* 133, no. 12 (2018): 527. https://doi.org/10.1140/epjp/i2018-12322-5
[13] Noor, Nur Azlina Mat, Sharidan Shafie, and Mohd Ariff Admon. "MHD squeezing flow of Casson nanofluid with chemical reaction, thermal radiation and heat generation/absorption." *Journal of Advanced Research in Fluid Mechanics and Thermal Sciences* 68, no. 2 (2020): 94-111. https://doi.org/10.37934/arfmts.68.2.94111
[14] Bhatti, M. M., A. Zeeshan, R. Ellahi, and G. C. Shit. "Mathematical modeling of heat and mass transfer effects on MHD peristaltic propulsion of two-phase flow through a Darcy-Brinkman-Forchheimer porous medium." *Advanced Powder Technology* 29, no. 5 (2018): 1189-1197. https://doi.org/10.1016/j.apt.2018.02.010
[15] Ellahi, R., A. Zeeshan, N. Shehzad, and Sultan Z. Alamri. "Structural impact of Kerosene-Al_2O_3 nanoliquid on MHD Poiseuille flow with variable thermal conductivity: application of cooling process." *Journal of Molecular Liquids* 264 (2018): 607-615. https://doi.org/10.1016/j.molliq.2018.05.103
[16] Alamri, Sultan Z., Ambreen A. Khan, Mariam Azeez, and R. Ellahi. "Effects of mass transfer on MHD second grade fluid towards stretching cylinder: a novel perspective of Cattaneo-Christov heat flux model." *Physics Letters A* 383, no. 2-3 (2019): 276-281. https://doi.org/10.1016/j.physleta.2018.10.035

[17] Mabood, F., R. G. Abdel-Rahman, and Giulio Lorenzini. "Effect of melting heat transfer and thermal radiation on Casson fluid flow in porous medium over moving surface with magnetohydrodynamics." *Journal of Engineering Thermophysics* 25 (2016): 536-547. https://doi.org/10.1134/S1810232816040111

[18] Hosseinzadeh, Kh, M. R. Mardani, M. Paikar, A. Hasibi, T. Tavangar, M. Nimafar, D. D. Ganji, and Mohammad Behshad Shafii. "Investigation of second grade viscoelastic non-Newtonian nanofluid flow on the curve stretching surface in presence of MHD." *Results in Engineering* 17 (2023): 100838. https://doi.org/10.1016/j.rineng.2022.100838

[19] Dinarvand, Saeed, Mahmoud Behrouz, Salar Ahmadi, Parsa Ghasemi, Samad Noeiaghdam, and Unai Fernandez-Gamiz. "Mixed convection of thermomicropolar AgNPs-GrNPs nanofluid: An application of mass-based hybrid nanofluid model." *Case Studies in Thermal Engineering* (2023): 103224. https://doi.org/10.1016/j.csite.2023.103224

[20] Rostami, H. Talebi, M. Fallah Najafabadi, Kh Hosseinzadeh, and D. D. Ganji. "Investigation of mixture-based dusty hybrid nanofluid flow in porous media affected by magnetic field using RBF method." *International Journal of Ambient Energy* 43, no. 1 (2022): 6425-6435. https://doi.org/10.1080/01430750.2021.2023041

[21] Dharmaiah, G., B. Shankar Goud, Nehad Ali Shah, and Muhammad Faisal. "Numerical analysis of heat and mass transfer with viscous dissipation, Joule dissipation, and activation energy." *International Journal of Ambient Energy* (2023): 1-13. https://doi.org/10.1080/01430750.2023.2224335

[22] Kumaran, G., and N. Sandeep. "Thermophoresis and Brownian moment effects on parabolic flow of MHD Casson and Williamson fluids with cross diffusion." *Journal of Molecular Liquids* 233 (2017): 262-269. https://doi.org/10.1016/j.molliq.2017.03.031

[23] Mohyud-Din, Syed Tauseef, Muhammad Usman, Wei Wang, and Muhammad Hamid. "A study of heat transfer analysis for squeezing flow of a Casson fluid via differential transform method." *Neural Computing and Applications* 30 (2018): 3253-3264. https://doi.org/10.1007/s00521-017-2915-x

[24] Reddy, M. Gnaneswara. "Unsteady radiative-convective boundary-layer flow of a Casson fluid with variable thermal conductivity." *Journal of Engineering Physics and Thermophysics* 88, no. 1 (2015): 240-251. https://doi.org/10.1007/s10891-015-1187-5

[25] Hussanan, Abid, Mohd Zuki Salleh, Ilyas Khan, and Sharidan Shafie. "Analytical solution for suction and injection flow of a viscoplastic Casson fluid past a stretching surface in the presence of viscous dissipation." *Neural Computing and Applications* 29 (2018): 1507-1515. https://doi.org/10.1007/s00521-016-2674-0

[26] Nadeem, Sohail, Rizwan Ul Haq, and Noreen Sher Akbar. "MHD three-dimensional boundary layer flow of Casson nanofluid past a linearly stretching sheet with convective boundary condition." *IEEE Transactions on Nanotechnology* 13, no. 1 (2013): 109-115. https://doi.org/10.1109/TNANO.2013.2293735

[27] Reyaz, Ridhwan, Yeou Jiann Lim, Ahmad Qushairi Mohamad, Muhammad Saqib, and Sharidan Shafie. "Caputo fractional MHD Casson fluid flow over an oscillating plate with thermal radiation." *Journal of Advanced Research in Fluid Mechanics and Thermal Sciences* 85, no. 2 (2021): 145-158. https://doi.org/10.37934/arfmts.85.2.145158

[28] Ramesh, G. K., B. J. Gireesha, S. A. Shehzad, and F. M. Abbasi. "Analysis of heat transfer phenomenon in magnetohydrodynamic Casson fluid flow through Cattaneo-Christov heat diffusion theory." *Communications in Theoretical Physics* 68, no. 1 (2017): 91. https://doi.org/10.1088/0253-6102/68/1/91

[29] Kumar, R. Naveen, RJ Punith Gowda, J. K. Madhukesh, B. C. Prasannakumara, and G. K. Ramesh. "Impact of thermophoretic particle deposition on heat and mass transfer across the dynamics of Casson fluid flow over a moving thin needle." *Physica Scripta* 96, no. 7 (2021): 075210. https://doi.org/10.1088/1402-4896/abf802

[30] Gudekote, Manjunatha, and Rajashekhar Choudhari. "Slip effects on peristaltic transport of Casson fluid in an inclined elastic tube with porous walls." *Journal of Advanced Research in Fluid Mechanics and Thermal Sciences* 43, no. 1 (2018): 67-80.

[31] Tawade, Jagadish V., C. N. Guled, Samad Noeiaghdam, Unai Fernandez-Gamiz, Vediyappan Govindan, and Sundarappan Balamuralitharan. "Effects of thermophoresis and Brownian motion for thermal and chemically reacting Casson nanofluid flow over a linearly stretching sheet." *Results in Engineering* 15 (2022): 100448. https://doi.org/10.1016/j.rineng.2022.100448

[32] Abo-Dahab, S. M., M. A. Abdelhafez, Fateh Mebarek-Oudina, and S. M. Bilal. "MHD Casson nanofluid flow over nonlinearly heated porous medium in presence of extending surface effect with suction/injection." *Indian Journal of Physics* (2021): 1-15. https://doi.org/10.1007/s12648-020-01923-z

[33] Mustafa, M., T. Hayat, I. Pop, and Al Aziz. "Unsteady boundary layer flow of a Casson fluid due to an impulsively started moving flat plate." *Heat Transfer-Asian Research* 40, no. 6 (2011): 563-576. https://doi.org/10.1002/htj.20358

[34] Mukhopadhyay, Swati, Iswar Chandra Mondal, and Ali J. Chamkha. "Casson fluid flow and heat transfer past a symmetric wedge." *Heat Transfer-Asian Research* 42, no. 8 (2013): 665-675. https://doi.org/10.1002/htj.21065

[35] Haq, Rizwan Ul, Sohail Nadeem, Zafar Hayat Khan, and Noreen Sher Akbar. "Thermal radiation and slip effects on MHD stagnation point flow of nanofluid over a stretching sheet." *Physica E: Low-Dimensional Systems and Nanostructures* 65 (2015): 17-23. https://doi.org/10.1016/j.physe.2014.07.013

[36] Hussain, Majid, Abdul Ghaffar, Akhtar Ali, Azeem Shahzad, Kottakkaran Sooppy Nisar, M. R. Alharthi, and Wasim Jamshed. "MHD thermal boundary layer flow of a Casson fluid over a penetrable stretching wedge in the existence of nonlinear radiation and convective boundary condition." *Alexandria Engineering Journal* 60, no. 6 (2021): 5473-5483. https://doi.org/10.1016/j.aej.2021.03.042

[37] Reddy, P. Bala Anki. "Magnetohydrodynamic flow of a Casson fluid over an exponentially inclined permeable stretching surface with thermal radiation and chemical reaction." *Ain Shams Engineering Journal* 7, no. 2 (2016): 593-602. https://doi.org/10.1016/j.asej.2015.12.010

[38] Oyelakin, Ibukun Sarah, Sabyasachi Mondal, and Precious Sibanda. "Unsteady Casson nanofluid flow over a stretching sheet with thermal radiation, convective and slip boundary conditions." *Alexandria Engineering Journal* 55, no. 2 (2016): 1025-1035. https://doi.org/10.1016/j.aej.2016.03.003

[39] Yusof, Nur Syamila, Siti Khuzaimah Soid, Mohd Rijal Illias, Ahmad Sukri Abd Aziz, and Nor Ain Azeany Mohd Nasir. "Radiative Boundary Layer Flow of Casson Fluid Over an Exponentially Permeable Slippery Riga Plate with Viscous Dissipation." *Journal of Advanced Research in Applied Sciences and Engineering Technology* 21, no. 1 (2020): 41-51. https://doi.org/10.37934/araset.21.1.4151

[40] Mahanthesh, Basavarajappa, Oluwole Daniel Makinde, Bijjanal Jayanna Gireesha, Koneri L. Krupalakshmi, and Isaac Lare Animasaun. "Two-phase flow of dusty Casson fluid with Cattaneo-Christov heat flux and heat source past a cone, wedge and plate." In *Defect and Diffusion Forum*, vol. 387, pp. 625-639. Trans Tech Publications Ltd, 2018. https://doi.org/10.4028/www.scientific.net/DDF.387.625

[41] Khan, Ansab Azam, Khairy Zaimi, Suliadi Firdaus Sufahani, and Mohammad Ferdows. "MHD flow and heat transfer of double stratified micropolar fluid over a vertical permeable shrinking/stretching sheet with chemical reaction and heat source." *Journal of Advanced Research in Applied Sciences and Engineering Technology* 21, no. 1 (2020): 1-14. https://doi.org/10.37934/araset.21.1.114

[42] Ibrahim, S. M., P. V. Kumar, G. Lorenzini, E. Lorenzini, and F. Mabood. "Numerical study of the onset of chemical reaction and heat source on dissipative MHD stagnation point flow of Casson nanofluid over a nonlinear stretching sheet with velocity slip and convective boundary conditions." *Journal of Engineering Thermophysics* 26 (2017): 256-271. https://doi.org/10.1134/S1810232817020096

[43] Gulzar, M. Mudassar, Anmol Aslam, M. Waqas, M. Asif Javed, and Kh Hosseinzadeh. "A nonlinear mathematical analysis for magneto-hyperbolic-tangent liquid featuring simultaneous aspects of magnetic field, heat source and thermal stratification." *Applied Nanoscience* 10 (2020): 4513-4518. https://doi.org/10.1007/s13204-020-01483-y

[44] Khan, Ansab Azam, Khairy Zaimi, Suliadi Firdaus Sufahani, and Mohammad Ferdows. "MHD Mixed Convection Flow and Heat Transfer of a Dual Stratified Micropolar Fluid Over a Vertical Stretching/Shrinking Sheet with Suction, Chemical Reaction and Heat Source." *CFD Letters* 12, no. 11 (2020): 106-120. https://doi.org/10.37934/cfdl.12.11.106120

[45] Yashkun, Ubaidullah, Fatinnabila Kamal, Khairy Zaimi, Nor Ashikin Abu Bakar, and Norshaza Atika Saidin. "Stability analysis on stagnation-point flow and heat transfer towards a permeable stretching/shrinking sheet with heat source in a Casson fluid." *CFD Letters* 12, no. 6 (2020): 1-15. https://doi.org/10.37934/cfdl.12.6.115

[46] Lanjwani, Hazoor Bux, M. Imran Anwar, M. Saleem Chandio, Sumera Dero, and Liaquat Ali Lund. "Magnetohydrodynamic (MHD) and Radiation Effect on the Casson Nanofluid flow over linear stretching sheet." *International Journal of Scientific & Engineering Research* 10, no. 4 (2019): 321-342.

[47] Nagasasikala, Madduleti, and Bommanna Lavanya. "Effects of dissipation and radiation on heat transfer flow of a convective rotating CuO-water Nano-fluid in a vertical channel." *Journal of Advanced Research in Fluid Mechanics and Thermal Sciences* 50, no. 2 (2018): 108-117.

[48] Bakar, Nor Ashikin Abu, Norfifah Bachok, and Norihan Md Arifin. "Nanofluid flow using Buongiorno model over a stretching sheet and thermophysical properties of nanoliquids." *Indian Journal of Science and Technology* 9 (2016): 1-9. https://doi.org/10.1063/1.4995849

[49] Yasmin, Humaira, and Zahid Nisar. "Mathematical Analysis of Mixed Convective Peristaltic Flow for Chemically Reactive Casson Nanofluid." *Mathematics* 11, no. 12 (2023): 2673. https://doi.org/10.3390/math11122673

[50] Ferdows, M., Md Shakhaoath Khan, Md Mahmud Alam, and A. A. Afify. "MHD boundary layer flow and heat transfer characteristics of a nanofluid over a stretching sheet." *Acta Universitatis Sapientiae, Mathematica* 9, no. 1 (2017): 140-161. https://doi.org/10.1515/ausm-2017-0009

[51] Ullah, Imran, Krishnendu Bhattacharyya, Sharidan Shafie, and Ilyas Khan. "Unsteady MHD mixed convection slip flow of Casson fluid over nonlinearly stretching sheet embedded in a porous medium with chemical reaction, thermal radiation, heat generation/absorption and convective boundary conditions." *PLoS One* 11, no. 10 (2016): e0165348. https://doi.org/10.1371/journal.pone.0165348

[52] Das, Mrutyunjay, Ganeswar Mahanta, and Sachin Shaw. "Heat and mass transfer effect on an unsteady MHD radiative chemically reactive Casson fluid over a stretching sheet in porous medium." *Heat Transfer* 49, no. 8 (2020): 4350-4369. https://doi.org/10.1002/htj.21830

[53] Deepika, A. R., K. Govardhan, Rafiuddin Mohammad, Hussain Basha, and G. Janardhana Reddy. "Dissipative magnetic ohmic heating influence on radiative nanofluid flow about a permeable stretching sheet under a porous medium with heat source." *International Journal of Ambient Energy* (2023): 1-12. https://doi.org/10.1080/01430750.2023.2224334

[54] Hsiao, Kai-Long. "Stagnation electrical MHD nanofluid mixed convection with slip boundary on a stretching sheet." *Applied Thermal Engineering* 98 (2016): 850-861. https://doi.org/10.1016/j.applthermaleng.2015.12.138